

Cross-Subject Data Splitting for Brain-to-Text Decoding

Anonymous ACL submission

Abstract

Recent major milestones have successfully decoded non-invasive brain signals (e.g. functional Magnetic Resonance Imaging (fMRI) and electroencephalogram (EEG)) into natural language. Despite the progress in model design, how to split the datasets for training, validating, and testing still remains a matter of debate. Most of the prior researches applied subject-specific data splitting, where the decoding model is trained and evaluated per subject. Such splitting method poses challenges to the utilization efficiency of dataset as well as the generalization of models. In this study, we propose a cross-subject data splitting criterion for brain-to-text decoding on various types of cognitive dataset (fMRI, EEG), aiming to maximize dataset utilization and improve model generalization. We undertake a comprehensive analysis on existing cross-subject data splitting strategies and prove that all these methods suffer from data leakage, namely the leakage of test data to training set, which significantly leads to overfitting and overestimation of decoding models. The proposed cross-subject splitting method successfully addresses the data leakage problem and we re-evaluate some SOTA brain-to-text decoding models as baselines for further research.

1 Introduction

Brain-to-text decoding aims to recover natural language from brain signals stimulated by corresponding speech. Recent studies (Makin et al., 2020; Wang and Ji, 2022; Xi et al., 2023; Tang et al., 2023; Duan et al., 2024) have successfully decoded non-invasive brain signals (e.g. fMRI, EEG) to text by applying deep computational neural networks. However, no consensus has reached on how to split the cognitive dataset for training, validating, and testing. Most of the prior work (Ye et al., 2023; Tang et al., 2023) performed subject-specific data splitting for training and evaluating decoding models. Under this splitting rule, data for training,

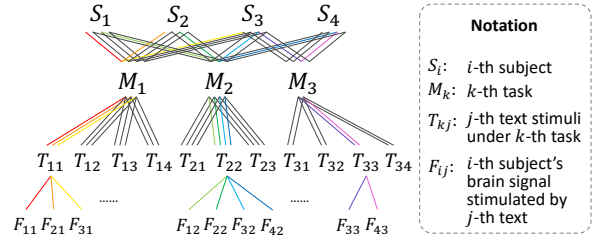


Figure 1: Illustration of naturalistic language comprehension dataset for brain-to-text decoding. Path with the same color indicates one sample for training/validating/testing.

validating, and testing all comes from one specific subject from the cognitive dataset. For example, Tang et al. (2023) picked three subjects out of seven and conducted model training and evaluation on the three subjects respectively. This subject-specific splitting method causes two main problems. First, it only utilizes a tiny part of the whole dataset. Since the collection of brain signals is costly and time-consuming, such splitting method results in significant waste of data resources. Second, it leads to the poor generalization of decoding models. As every subject's brain has unique functional and anatomical structures, subject-specific models may exhibit considerable variability across individuals and fail to generalize to other subjects. Moreover, decoding models trained from scratch on limited data are prone to facing the overfitting problem.

Some studies (Wang and Ji, 2022; Xi et al., 2023) began to shed light on cross-subject data splitting, which views all the subjects' data as a whole and performs splitting according to a given ratio (e.g. 8:1:1 for the training set, validation set, and test set). Cross-subject data splitting effectively compensates for the shortcomings of subject-specific splitting and has been widely applied in brain-to-image decoding (Wang et al., 2024; Liu et al., 2024). However, unlike datasets for brain-to-image decoding, where subjects are guided to see different and unrepeated pictures, different subjects will hear

072 the same story in the naturalistic language compre- 123
073 hension dataset for brain-to-text decoding, which 124
074 challenges cross-subject data splitting. As shown 125
075 in Figure 1, such dataset is usually formatted in 126
076 subject-task-text-signal (S - M - T - F) pair, indicat- 127
077 ing the brain signal F of subject S stimulated by 128
078 hearing text T from task M . Current cross-subject 129
079 data splitting methods (Wang and Ji, 2022; Xi et al., 130
080 2023) can be summarized as five categories: (1) 131
081 split by subjects S , (2) split by tasks M , (3) split 132
082 by randomly picking signal frames F , (4) split by 133
083 randomly picking signal frames under certain task 134
084 F - M , (5) split by randomly picking consecutive 135
085 signal frames under certain task F - M . However, 136
086 based on our observations, all these splitting meth- 137
087 ods suffer from **data leakage** problem, namely part 138
088 of the test data is mixed into the training set, which 139
089 leads to overfitting in model training and overesti-
090 mation in model evaluation.

091 Specifically, modern brain-to-text decoding mod- 141
092 els follow an encoder-decoder manner. We pick 142
093 two representative models: EEG2Text (Wang and 143
094 Ji, 2022) and UniCoRN (Xi et al., 2023) for investi- 144
095 gating the damage of data leakage. The former is an 145
096 end-to-end encoder-decoder framework, while the 146
097 latter first pre-trains the encoder and then applies 147
098 it in the decoder training. Experiments support 148
099 that data leakage affects model training on both 149
100 the encoder side and decoder side. For the encoder 150
101 component, if subjects’ brain signals in the test set 151
102 are mixed into the training set, the encoder will be- 152
103 come overfitting and fail to well represent unseen 153
104 subjects’ brain signals. As to the decoder, the situ- 154
105 ation gets worse if text stimuli are leaked. Since 155
106 the decoder follows an auto-regressive manner and 156
107 generates token by token, data leakage will cause 157
108 the decoder to memorize seen paragraphs during 158
109 the teacher-forcing training stage, which leads to 159
110 poor generalization to unseen text. 160

111 To avoid data leakage and fairly evaluate the 161
112 performance of brain-to-text decoding models, we 162
113 propose a cross-subject data splitting criterion. We 163
114 focus on fMRI and EEG signals in this study, al- 164
115 though the proposed criterion could be applied to 165
116 any datasets satisfying the prescribed format. In 166
117 the proposed method, the dataset is split according 167
118 to subject-text (S - T) pairs with the following rules: 168
119 (1) Brain signals collected from specific subject in 169
120 validation set and test set will not appear in train- 170
121 ing set, which means the trained encoder cannot 171
122 get access to any brain information belonging to 172

123 subjects in test set. (2) Text stimuli in validation 124
125 set and test set will not appear in training set. The 126
127 decoder learns to reconstruct language with brain 128
129 signals instead of memorizing seen text. 130

131 Our contributions can be summarized as follows: 132

- 133 • To the best of our knowledge, we propose the 134
135 first cross-subject data splitting criterion for 136
137 brain-to-text decoding. 138
- 139 • We comprehensively analyze current cross-
140 subject data splitting methods and find that
141 all existing methods suffer from data leakage
142 problem, which severely affects the training
143 and evaluation of decoding models. 144
- 145 • Some SOTA brain-to-text decoding models
146 are re-evaluated under the proposed cross-
147 subject data splitting method as baselines for
148 further research. 149

150 2 Related Work 151

152 **Brain Signal** Brain signals can be classified into 153
154 three categories: invasive, partially invasive, and 155
156 non-invasive according to how close electrodes get 157
158 to brain tissue. In this paper, we mainly focus on 159
160 non-invasive signals EEG and fMRI. EEG signal 161
162 is electrogram of the spontaneous electrical activ- 163
164 ity of the brain, with frequencies ranging from 1 164
165 Hz to 30 Hz. EEG is of high temporal resolution 165
166 and relatively tolerant of subject movement, but its 166
167 spatial resolution is low and it can’t display active 167
168 areas of the brain directly. fMRI measures brain 168
169 activity by detecting changes of blood flow. Blood 169
170 flow of a specific region increases when this brain 170
171 area is in use. The spatial resolution of fMRI is 171
172 measured by the size of voxel, which is a three-
dimensional rectangular cuboid ranging from 3mm
to 5mm (Vouloumanos et al., 2001; Noppeney and
Price, 2004). Unlike EEG which samples brain sig-
nals continuously, fMRI samples based on a fixed
time interval named TR, usually at second level.

173 **Brain-to-text Decoding** Previous research on 174
175 brain-to-text decoding (Herff et al., 2015; Anu- 175
176 manchipalli et al., 2019; Zou et al., 2021; Moses 176
177 et al., 2021; Défossez et al., 2023) mainly focused 177
178 on word-level decoding in a restricted vocabulary 178
179 with hundreds of words (Panachakel and Ramakr- 179
180 ishnan, 2021). These models typically apply re- 180
181 current neural network or long short-term memory 181
182 (Hochreiter and Schmidhuber, 1997) network to 182
183 build mapping between brain signals and words 183
184 in vocabulary. Despite relatively good accuracy, 184
185 these methods fail to generalize to unseen words. 185

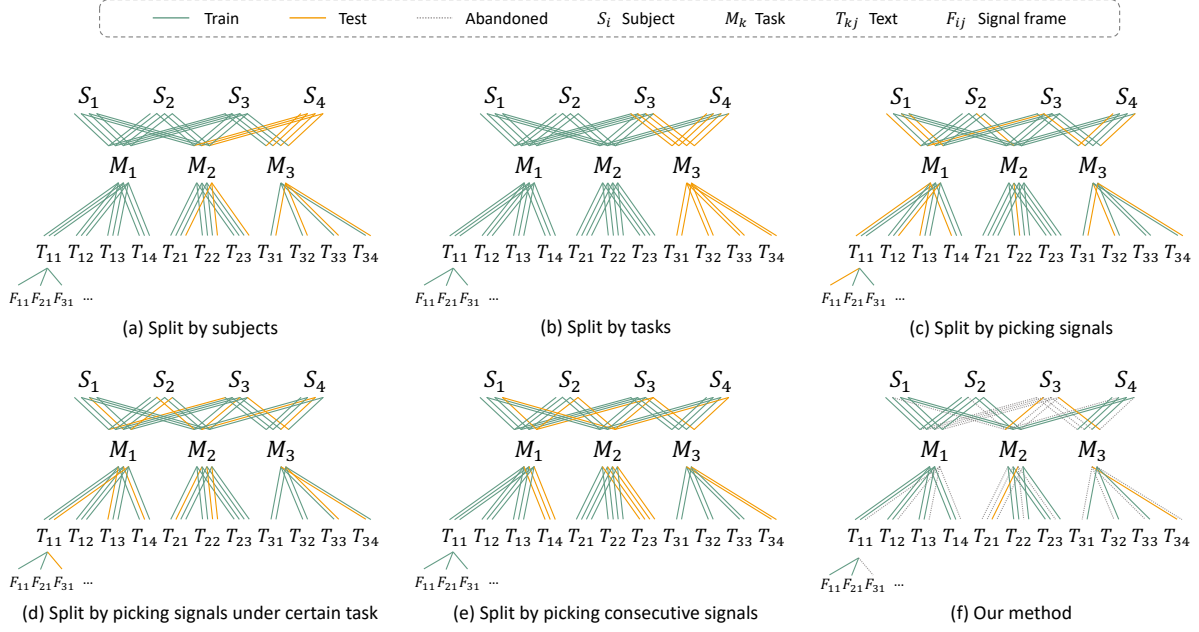


Figure 2: Different splitting methods for cognitive dataset. (Color printing is preferred.)

Some progress (Sun et al., 2019) has been made by expanding word-level decoding to sentence-level through encoder-decoder framework or using less noisy ECoG data (Burle et al., 2015; Anumanchipalli et al., 2019). However, these models struggle to generate accurate and fluent sentences limited by decoder ability. Wang and Ji (2022) introduced the first open vocabulary EEG-to-text decoding model by leveraging the power of pre-trained language models. Xi et al. (2023) improved the model design and proposed a unified framework for decoding both fMRI and EEG signals.

3 Methodology

In this section, we will first introduce the formal definition of brain-to-text decoding and the general description of dataset format. Then we systematically analyze current cross-subject data splitting methods and point out that all existing methods suffer from two kinds of data leakage issues: brain signal leakage and text stimuli leakage. Finally, a cross-subject splitting criterion is proposed which avoids the above-mentioned data leakage problems.

3.1 Task Definition

Given the brain signal F_{ij} stimulated by i -th subject S_i hearing or reading certain text T_j , brain-to-text decoding aims to decode F_{ij} back to text T'_j and make T'_j as similar as possible to T_j . The composition of F_{ij} and T_j is different as to fMRI and

EEG. The former samples brain information discretely with a fixed time interval TR, while the latter samples continuously. To fMRI, consistent text segments s_j with corresponding fMRI frames f_{ij} are concatenated to form a sample pair $\langle F_{ij}, T_j \rangle$, where $T_j = \text{concat}(s_j, s_{j+1}, \dots, s_{j+L-1})$ and $F_{ij} = \text{concat}(f_{ij}, f_{i,j+1}, \dots, f_{i,j+L-1})$, and $|T_j| = |F_{ij}| = L$. To EEG, since signals corresponding to complete text stimuli are available and they are continuous, we bond text T_j (i.e. text stimuli) and EEG signal F_{ij} together to form a sample pair $\langle F_{ij}, T_j \rangle$. Under most scenarios, each text stimulus T_j belongs to one certain task M_k . So the signal-text pair $\langle F_{ij}, T_j \rangle$ can be further split into $\langle F_{ij}, M_k \rangle$ and $\langle M_k, T_{kj} \rangle$.

One of the purposes of cross-subject splitting is to endow models the ability to decode unseen subject's brain signal. As a result, if brain signal F_{ij} appears in test set S_{test} , any signal F_{i^*} belonging to subject i should not appear in training set S_{train} . Similarly, text stimuli T_{kj} in S_{test} should not appear in S_{train} . The above splitting rules for training set can be formulated by Cartesian product:

$$S_{train} = F_{train} \times T_{train}, \quad (1)$$

where

$$F_{train} = \{F_{ij} | i \in I\}, \quad (2)$$

$$I = \{i | F_{ij} \notin S_{val}, S_{test}, \forall j\}, \quad (3)$$

and

$$T_{train} = \{T_{kj} | T_{kj} \notin S_{val}, S_{test}\}. \quad (4)$$

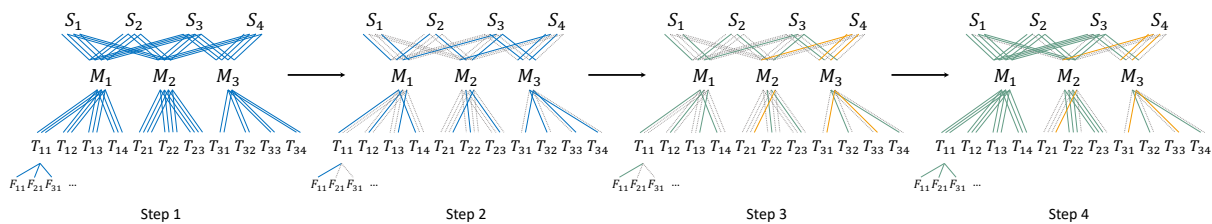


Figure 3: The process of our proposed cross-subject data splitting method. (Color printing is preferred.)

Such rules are also applicable to validation and test set. We omit their displays here for simplicity.

3.2 Current Splitting Methods

Current cross-subject data splitting methods can be summarized as five categories according to classifying objectives S_i, M_k, T_{kj}, F_{ij} . More specifically, the five dataset splitting methods are characterised as (1) split by subjects S_i , (2) split by tasks M_k , (3) split by randomly picking signal frames F_{ij} , (4) split by randomly picking signal frames under certain task $F_{ij}-M_k$, (5) split by randomly picking consecutive signal frames under certain task $F_{ij}-M_k$, corresponding to (a), (b), (c), (d), (e) in Figure 2. Figure 2 vividly displays the differences between current dataset splitting methods. In this example, we choose 4 subjects (S_1 to S_4) with 3 tasks (M_1 to M_3) each containing 4 (T_{11} to T_{14}), 3 (T_{21} to T_{23}), 4 (T_{31} to T_{34}) text stimuli respectively. F_{ij} indicates the brain signal of i -th subject stimulated by j -th text under task M_k , e.g. F_{21} means brain signal of S_2 hearing T_{11} .

The line connecting two symbols indicates they are related to one sample in dataset. Take path S_1, M_1, T_{11}, F_{11} for example, it indicates that subject S_1 listens to text stimuli T_{11} belonging to task M_1 and S_1 's corresponding brain signal is recorded as F_{11} . Some symbols are connected with several lines. For example, the four lines between S_1 and M_1 correspond to $\langle M_1, T_{11} \rangle, \langle M_1, T_{12} \rangle, \langle M_1, T_{13} \rangle, \langle M_1, T_{14} \rangle$ counting from left to right. Similarly, the three lines between M_1 and T_{11} correspond to $\langle S_1, M_1 \rangle, \langle S_2, M_1 \rangle, \langle S_3, M_1 \rangle$ respectively. The same rules can be extended to other lines and symbols. The green lines and orange lines stand for training samples and testing samples. The grey dotted line means the sample is abandoned, which will be introduced in our data splitting method. As the splitting of validation set is the same as test set, we only consider training set and test set in this section for simplicity.

We will use method (a), (b), (c), (d), (e) to represent five current dataset splitting methods in the rest of the paper. Method (a) splits the dataset according to **subjects**, which can be described as

$$S_{train} = \{ \langle F_{ij}, T_{kj} \rangle \mid S_i \notin S_{val}, S_{test} \} \quad (5)$$

for training set. Method (b) splits the dataset according to **tasks**, which is described as

$$S_{train} = \{ \langle F_{ij}, T_{kj} \rangle \mid M_k \notin S_{val}, S_{test} \} \quad (6)$$

for training set. Method (c), (d), and (e) all split the dataset according to **brain signal frames**

$$S_{train} = \{ \langle F_{ij}, T_{kj} \rangle \mid F_{ij} \notin S_{val}, S_{test} \}. \quad (7)$$

However, there are slight differences between these three methods. Method (c) views all the brain signal frames in dataset as a whole and splits according to the default proportion (e.g. 8:1:1). Method (d) views signal frames under certain task M_k as a whole and splits proportionally, and then unions all training sets under different tasks to form a complete set for training. Method (e) is similar to method (d). They both first split training, validation, and test set under certain task proportionally and then union them. The difference lies in that method (d) randomly picks signal frames, while method (e) picks consecutive signal frames.

We first point out the data leakage problems in current splitting methods through the analysis of training set and test set composition. Specifically, following the definition in subsection 3.1, two kinds of data leakage, *brain signal leakage* and *text stimuli leakage*, are defined. The data leakage situation of different methods can be reflected through visualization in Figure 2. Lines between S_i and M_k indicate brain signal leakage situation and lines between T_{kj} and M_k indicate text stimuli leakage situation. If lines associated with S_i or T_{kj} are of different colours, data in test set leaks into training set. Remind the composition of samples

| Type | Method | Narratives / ZuCo | | | | Average |
|---------|--------|---------------------|---------------------|---------------------|---------------------|---------------------|
| | | seed1 | seed2 | seed3 | seed4 | |
| BSLR(%) | (a) | 0.00 / 0.00 | 0.00 / 0.00 | 0.00 / 0.00 | 0.00 / 0.00 | 0.00 / 0.00 |
| | (b) | 6.73 / - | 6.32 / - | 7.7 / - | 17.93 / - | 9.67 / - |
| | (c) | 12.55 / 12.52 | 12.52 / 12.55 | 12.48 / 12.48 | 12.44 / 12.46 | 12.50 / 12.50 |
| | (d) | 12.81 / 12.60 | 12.8 / 12.58 | 12.78 / 12.56 | 12.79 / 12.61 | 12.795 / 12.59 |
| | (e) | 12.28 / - | 12.27 / - | 12.26 / - | 12.27 / - | 12.27 / - |
| | (f) | 0.00 / 0.00 | 0.00 / 0.00 | 0.00 / 0.00 | 0.00 / 0.00 | 0.00 / 0.00 |
| TSLR(%) | (a) | 100.00 / 23.43 | 100.00 / 20.25 | 100.00 / 23.38 | 100.00 / 22.95 | 100.00 / 22.50 |
| | (b) | 0.00 / - | 0.00 / - | 0.00 / - | 0.00 / - | 0.00 / - |
| | (c) | 100.00 / 13.21 | 100.00 / 13.06 | 100.00 / 12.91 | 100.00 / 13.1 | 100.00 / 13.07 |
| | (d) | 99.93 / 0.00 | 99.81 / 0.00 | 99.54 / 0.00 | 99.99 / 0.00 | 99.82 / 0.00 |
| | (e) | 9.19 / - | 9.31 / - | 9.36 / - | 9.29 / - | 9.29 / - |
| | (f) | 0.00 / 0.00 | 0.00 / 0.00 | 0.00 / 0.00 | 0.00 / 0.00 | 0.00 / 0.00 |

Table 1: Results of Brain Signal Leakage Rate (BSLR) and Text Stimuli Leakage Rate (TSLR).

differs as to fMRI signal and EEG signal, so the dataset splitting methods are different for two kinds of brain signal too. Since fMRI signals need to be sampled continuously with a certain length L , one sample shown in Figure 2 (e.g. $S_1-M_1-T_{11}-F_{11}$) is actually the first part of one fMRI sample, with $L-1$ continuous brain signal frames following (e.g. F_{12}, F_{13}, \dots). In this sense, brain signal leakage doesn't exist in method (a) for EEG, but method (a) suffers from text stimuli leakage. Text stimuli leakage does not exist in method (b) but brain signal leakage exists. Method (c) suffers from both brain signal leakage and text stimuli leakage. Method (d) and (e) are the same to EEG, with brain signal leakage. For fMRI, the situation of data leakage for different methods is similar to EEG, except for method (d) and (e), which are the same for EEG but actually different for fMRI. Method (d) suffers from both brain signal leakage and text stimuli leakage while in method (e) text stimuli leakage happens in the overlap between training samples and test samples.

3.3 Cross-Subject Splitting Criterion

To eliminate data leakage from both brain signal leakage and text stimuli leakage, we split the dataset by $\langle S_i, T_j \rangle$ pairs as shown in (f) of Figure 2. Since EEG and fMRI are different in the composition of dataset, we treat them separately and propose two data splitting methods. As to EEG dataset where F_{ij} and T_j form a sample, we consider a bipartite graph $\mathcal{G}_1 = (\mathcal{U}, \mathcal{V}, \mathcal{E})$ where $\mathcal{U} = \{S_i\}_{i=1}^N$, $\mathcal{V} = \{T_j\}_{j=1}^M$. \mathcal{E} is the edge between node in \mathcal{U} and node in \mathcal{V} , indicating $\langle S_i, T_j \rangle$ pair in the dataset.

N is the total number of subjects and M is the total number of unique text stimuli. We assert $M > N$, so $e = (u, v) \in \mathcal{E}$ exists for every $v \in \mathcal{V}$, as each text stimuli is listened or read by at least one subject. As shown in step 2 of Figure 3, first we pick one edge for each node $v \in \mathcal{V}$ and build a new bipartite graph $\mathcal{G}_2 = (\mathcal{U}, \mathcal{V}, \mathcal{E}')$. Then following step 3, we split graph \mathcal{G}_2 by subject \mathcal{U} with the given splitting ratio and form three disjoint graphs $\mathcal{G}_{train}, \mathcal{G}_{val}, \mathcal{G}_{test}$. In step 4, some edges satisfying zero data leakage condition are not included in the graph. We add these edges to corresponding graphs, extending each graph $\mathcal{G}_{train}, \mathcal{G}_{val}, \mathcal{G}_{test}$ to its maximally scalable state and finishing the dataset splitting process.

The sample in fMRI dataset is formatted in $F_{ij} = \text{concat}(f_{ij}, f_{i,j+1}, \dots, f_{i,j+L-1})$ and $T_j = \text{concat}(s_j, s_{j+1}, \dots, s_{j+L-1})$. If we follow the same process as EEG, text stimuli leakage will occur in the overlapping part of two samples, when one sample is assigned to training set and the other is assigned to validation or test set. We propose a simple solution that achieves the balance between abandoning as little data as possible and ensuring zero data leakage. Instead of $\langle S_i, T_j \rangle$ pair, we consider $\langle S_i, M_k \rangle$ pair and apply the above-mentioned algorithm. More details and pseudo-code are available in Appendix B.

4 Experimental Settings

We test some SOTA brain-to-text decoding models on two popular cognitive datasets Narratives (Nastase et al., 2021) and ZuCo (Hollenstein et al.,

| Model | Epoch+lr+Method | BLEU-N (%) | | | | ROUGE-1 (%) | | |
|----------|-----------------|--------------|--------------|--------------|--------------|--------------|--------------|--------------|
| | | $N = 1$ | $N = 2$ | $N = 3$ | $N = 4$ | R | P | F |
| UniCoRN | 10+1e-3+(a) | 49.56 | 30.49 | 21.07 | 15.49 | 44.83 | 50.41 | 40.65 |
| | 10+1e-3+(b) | 26.37 | 7.50 | 2.48 | 0.99 | 22.28 | 25.99 | 19.62 |
| | 10+1e-3+(c) | 50.24 | 30.83 | 21.23 | 15.60 | 44.68 | 49.44 | 41.01 |
| | 10+1e-3+(d) | 49.63 | 30.29 | 20.85 | 15.32 | 45.06 | 50.47 | 41.03 |
| | 10+1e-3+(e) | 28.94 | 9.39 | 4.07 | 1.53 | 21.68 | 24.64 | 19.49 |
| UniCoRN* | 20+1e-4+(a) | 50.19 | 34.25 | 25.98 | 21.00 | 46.59 | 50.36 | 43.62 |
| | 30+1e-4+(a) | 55.46 | 40.99 | 32.85 | 27.56 | 52.08 | 55.02 | 49.68 |
| | 20+1e-4+(b) | 25.91 | 8.80 | 3.84 | 1.66 | 20.65 | 27.74 | 16.57 |
| | 30+1e-4+(b) | 25.91 | 8.80 | 3.84 | 1.66 | 20.65 | 27.74 | 16.57 |
| | 20+1e-4+(c) | 72.44 | 60.84 | 53.35 | 47.88 | 70.52 | 74.10 | 67.53 |
| | 30+1e-4+(c) | 72.82 | 61.42 | 53.95 | 48.44 | 71.24 | 74.41 | 68.57 |
| | 20+1e-4+(d) | 65.31 | 51.02 | 42.54 | 36.72 | 62.76 | 67.09 | 59.29 |
| | 30+1e-4+(d) | 66.56 | 53.00 | 44.75 | 39.02 | 63.89 | 67.51 | 60.95 |
| | 20+1e-4+(e) | 32.15 | 12.34 | 5.57 | 2.45 | 24.28 | 30.43 | 20.35 |
| | 30+1e-4+(e) | 32.15 | 12.34 | 5.57 | 2.45 | 24.28 | 30.43 | 20.35 |

Table 2: Generation quality of UniCoRN model for fMRI under different training settings. Here UniCoRN* indicates the encoder of UniCoRN is randomly initialized instead of pre-trained through signal reconstruction task.

2018). Dataset details are introduced in Appendix A. Comprehensive experiments are conducted to evidence the existence of the following phenomena: (1) Brain signals and text stimuli in test set leak into training set in all current dataset splitting methods. (2) The model’s generalization ability, particularly that of the auto-regressive decoder, has been overestimated due to data leakage. Because the number of tasks in EEG dataset is too small and method (e) makes no difference to EEG as method (d), we only consider method (a), (c), (d) for EEG.

4.1 Implementation

We follow the same settings of UniCoRN (Xi et al., 2023) and EEG2Text (Wang and Ji, 2022), except all the datasets are split to the ratio of 8:1:1 for fair comparison. All experiments are conducted on NVIDIA A100-SXM4-40GB GPUs. More details are shown in Appendix A.

4.2 Data Leakage Metrics

We have analyzed two kinds of data leakage: brain signal leakage and text stimuli leakage in section 3. In this part, we will quantify two kinds of data leakage through experiments.

To better illustrate the extent of data leakage of different data splitting methods, we design two novel evaluation metrics named **Brain Signal**

Leakage Rate (BSLR) and **Text Stimuli Leakage Rate (TSLR)** for detecting brain signal leakage and text stimuli leakage. Note that the situation for validation set is the same as test set, so we only consider test set in experiments. BSLR indicates the average percentage of each subject’s brain signals in test set appearing in training set, which could be formulated as

$$\frac{1}{N} \sum_{i=1}^N \min(1, \frac{|\{F_{ij}|F_{ij} \in S_{test} \cap S_{train}\}|}{|\{F_{ij}|F_{ij} \in S_{train}\}|}) \quad (8)$$

where N stands for the total number of subjects in test set. $|\cdot|$ stands for the cardinality of a set. Function $\min(\cdot, \cdot)$ is applied to make sure for each subject the data leakage rate is less than one.

The definition of TSLR is somewhat different for EEG signal and fMRI signal. As to EEG signal where brain signals are sampled continuously, it’s easy to match certain text stimuli with corresponding signals. Its TSLR is similar to BSLR, which indicates the average percentage of certain text in test set appearing in training set. TSLR for EEG data can be calculated through

$$\frac{1}{M} \sum_{j=1}^M \min(1, \frac{|\{T_{ij}|T_{ij} \in S_{test} \cap S_{train}\}|}{|\{T_{ij}|T_{ij} \in S_{train}\}|}) \quad (9)$$

where M stands for the total number of unique text

| Model | Epoch+lr+Method | BLEU-N (%) | | | | ROUGE-1 (%) | | |
|----------|-----------------|--------------|--------------|--------------|--------------|--------------|--------------|--------------|
| | | $N = 1$ | $N = 2$ | $N = 3$ | $N = 4$ | R | P | F |
| UniCoRN | 50+1e-4+(a) | 58.09 | 49.23 | 43.23 | 38.43 | 63.88 | 61.12 | 67.50 |
| | 80+1e-4+(a) | 60.88 | 50.52 | 43.42 | 37.84 | 65.17 | 61.16 | 70.72 |
| | 50+1e-4+(c) | 52.30 | 42.89 | 36.80 | 32.17 | 57.39 | 51.09 | 67.29 |
| | 80+1e-4+(c) | 60.78 | 55.92 | 53.18 | 51.10 | 84.64 | 63.16 | 71.50 |
| | 50+1e-4+(d) | 22.90 | 7.36 | 2.71 | 0.95 | 17.73 | 19.90 | 17.33 |
| | 80+1e-4+(d) | 22.90 | 7.36 | 2.71 | 0.95 | 17.73 | 19.90 | 17.33 |
| | 50+1e-4+(a) | 51.22 | 33.83 | 22.99 | 16.05 | 46.40 | 46.85 | 46.58 |
| | 80+1e-4+(a) | 63.32 | 52.52 | 45.19 | 39.50 | 65.96 | 64.74 | 68.01 |
| EEG2Text | 50+1e-4+(c) | 53.83 | 38.99 | 29.57 | 23.01 | 53.64 | 54.19 | 53.56 |
| | 80+1e-4+(c) | 65.42 | 57.56 | 52.56 | 48.60 | 73.00 | 69.99 | 77.01 |
| | 50+1e-4+(d) | 23.92 | 8.16 | 3.21 | 1.20 | 20.78 | 19.96 | 23.89 |
| | 80+1e-4+(d) | 23.92 | 8.16 | 3.21 | 1.20 | 20.78 | 19.96 | 23.89 |

Table 3: Generation quality of UniCoRN and EEG2Text model for EEG under different training settings.

periods in test set and T_{ij} stands for j -th period of text stimuli received by i -th subject.

The fMRI signal is sampled discretely with a deterministic interval TR, making it hard to acquire signals corresponding to text. Previous methods instead concatenated continuous fMRI frames of certain length with their corresponding text segments as training samples. As a result, we consider the average percentage of the same text segments in test set appearing in training set as TSLR for fMRI signal. It can be formulated as

$$\frac{1}{M} \sum_{j=1}^M \tau \frac{|\{T_{ij}|T_{ij} \in S_{test} \cap S_{train}\}|}{|S_{test}| \times L} \quad (10)$$

where $\tau = 0$ if $\{T_{ij}|T_{ij} \in S_{test} \cap S_{train}\} = \emptyset$ else

$$\tau = \min(1, \frac{|\{T_{ij}|T_{ij} \in S_{train}\}|}{|\{T_{ij}|T_{ij} \in S_{test} \cap S_{train}\}|}). \quad (11)$$

5 Results and Analysis

5.1 Verification for Data Leakage

We test current data splitting methods and our method on fMRI dataset ‘‘Narratives’’ and EEG dataset ZuCo. Considering the influence of randomness in splitting, we randomly select four seeds for experiments. The results are shown in Table 1, and are consistent with theoretical analysis. For fMRI, current methods apart from method (a) suffer from brain signal leakage, while method (a) has serious text stimuli leakage. Method (b) gets

no text stimuli leakage but has slight brain signal leakage. The situation for EEG is similar to that of fMRI. Apart from our proposed method (f), there is no way to achieve zero brain signal leakage and text stimuli leakage at the same time.

5.2 Damage of Data Leakage

Brain signal leakage and text stimuli leakage will damage brain-to-text decoding models from both the encoder side and decoder side.

Effect on Encoder The encoder of current brain-to-text decoding models can be trained in two ways: either jointly with the decoder or solely pre-trained through a reconstruction task. In the former end-to-end training scenario, it is hard to evaluate encoder performance separately. So we mainly focus on the latter, in which case the encoder is pre-trained through an encoder-decoder framework to reconstruct input brain signals. The decoder here does not refer to the decoder for text generation. It is similar to the structure of the encoder and will be abandoned once the encoder is pre-trained. Since a proper evaluation index of the encoder’s representation ability is missing, validation loss is applied to measure the effect of data leakage.

We test different splitting methods on two cognitive datasets. The validation loss of encoder is shown in Figure 4. For fMRI, influenced by leakage of brain signals, the validation loss of method (b), (c), (d), (e) keeps dropping even with long training epochs. The encoder is actually overfitting and

| Dataset | Model | BLEU-N (%) | | | | ROUGE-1 (%) | | |
|------------|----------|--------------|-------------|-------------|-------------|--------------|--------------|--------------|
| | | $N = 1$ | $N = 2$ | $N = 3$ | $N = 4$ | R | P | F |
| Narratives | UniCoRN | 22.83 | 5.69 | 1.43 | 0.48 | 15.55 | 24.80 | 19.04 |
| ZuCo | UniCoRN | 23.32 | 7.78 | 3.01 | 1.09 | 18.47 | 20.00 | 17.92 |
| | EEG2Text | 24.49 | 7.49 | 2.28 | 0.62 | 23.98 | 23.95 | 25.74 |

Table 4: A fair benchmark for evaluating brain-to-text decoding.

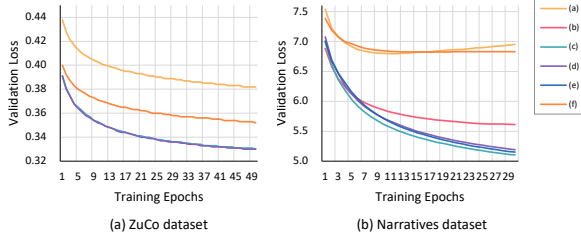


Figure 4: Validation loss of encoder under different dataset splitting methods in two datasets.

degrading. For method (a) and (f) without brain signal leakage, the validation loss quickly rises after reaching the lowest point with a few epochs, satisfying the basic rule of machine learning. For EEG, we find validation loss keeps dropping for all methods even with very long training epochs, regardless of brain signal leakage or not. We think the poor spatial resolution of EEG signal might lead to this phenomenon.

Effect on Decoder All SOTA models choose the pre-trained language model BART (Lewis et al., 2020) as decoder. The powerful model is able to achieve fluent open vocabulary text generation. However, if data leakage occurs, due to the autoregressive generation that calculates the probability of current token based on all previous tokens, the decoder will generate seen text given the first few words, and fail to generalize to unseen text.

The influence of text stimuli leakage on decoder is detected through BLEU scores (Papineni et al., 2002) and ROUGE-1 scores (Lin, 2004), which measure text similarity between generated text and ground truth. If evaluation indicators keep improving as training epochs increase, we believe part of the test set is leaked into training set and the model is overfitting. For fMRI signal, we test five current dataset splitting methods under different training settings. As shown in Table 2, we test two kinds of UniCoRN models. One is UniCoRN with finely tuned hyper-parameters claimed in the original paper, and the other is UniCoRN* with a randomly

initialized encoder. Empirically, the former will perform much better than the latter. However, in method (a), (c), (d), due to text stimuli leakage, if we reduce the learning rate and extend training epochs, UniCoRN* performs much better than UniCoRN and its performance keeps rising with longer training epochs. As to method (b) and (e) with no text stimuli leakage, changing training epochs or learning rates makes no obvious difference to model performance. For EEG signal, the conclusion is similar as shown in Table 3. For method (a) and (c) with text stimuli leakage, model performance keeps rising with longer training epochs. For method (d) without text stimuli leakage, both models reach optimal performance after the first few rounds of training epochs.

5.3 A Fair Benchmark

We re-evaluate current SOTA models for brain-to-text decoding under our cross-subject data splitting method and release a fair benchmark. UniCoRN is tested for both fMRI and EEG decoding, EEG2Text model is tested for EEG decoding. The results are listed in Table 4. For EEG dataset, UniCoRN achieves higher results in BLEU-2,3,4 while EEG2Text is better in BLEU-1 and ROUGE-1.

6 Conclusion

In this paper, we conduct a comprehensive study on existing cross-subject data splitting methods, and evidence that all these methods suffer from data leakage problem. Such data leakage largely exaggerates model performance and leads to poor generalization. To fix this issue, we propose a cross-subject data splitting criterion for brain-to-text decoding, aiming to improve the utilization efficiency of cognitive dataset and the generalization ability of decoding models. Experiments are conducted on fMRI and EEG dataset respectively. Current SOTA models are re-evaluated under this proposed splitting method and a fair benchmark is released for further research in this domain.

548 Limitations

549 The “Narratives” dataset and the ZuCo dataset provide researchers with precise brain signal resources
550 stimulated by text or voice. However, in the brain-to-text decoding task, both subject’s brain signals
551 and text stimuli in the validation and test set need to be invisible to the training set, which makes splitting
552 these public datasets difficult. Our proposed dataset splitting method meets the above requirements at the expense of discarding some data in
553 the dataset. We recommend future datasets in this domain follow these guidelines. The division of
554 the training set, validation set, and test set should be provided when the dataset is released. Besides,
555 we suggest hiring new subjects with unique stimuli for the validation set and test set, which is good for
556 testing the generalization ability of models without loss of data. What’s more, we find existing models
557 rely more on a strong auto-regressive decoder to achieve good generation quality. The encoder is of
558 limited use in all SOTA models. And we also notice in experiments that the encoder of EEG2Text keeps
559 overfitting whether with or without brain signal leakage. We leave it to research in the future.
570
571

572 Ethics Statement

573 In this paper, we introduce a new dataset splitting method to avoid data leakage for decoding brain
574 signals to text task. Experiments are conducted on the publicly accessible cognitive datasets “Narratives”
575 and ZuCo1.0 with the authorization from their respective maintainers. Both datasets have been de-identified
576 by dataset providers and used for researches only.
577
578
579
580

581 References

582 Gopala K Anumanchipalli, Josh Chartier, and Edward F Chang. 2019. Speech synthesis from neural decoding
583 of spoken sentences. *Nature*, 568(7753):493–498.
584
585 Boris Burle, Laure Spieser, Clémence Roger, Laurence Casini, Thierry Hasbroucq, and Franck Vidal. 2015.
586 Spatial and temporal resolutions of eeg: Is it really black and white? a scalp current density view. *International Journal of Psychophysiology*, 97(3):210–
587 220.
588
589 Yiqun Duan, Charles Chau, Zhen Wang, Yu-Kai Wang, and Chin-teng Lin. 2024. Dewave: Discrete encoding
590 of eeg waves for eeg to text translation. *Advances in Neural Information Processing Systems*, 36.
591
592 Alexandre Défossez, Charlotte Caucheteux, Jérémy Rapin, Ori Kabeli, and Jean-Rémi King. 2023.

597 [Decoding speech perception from non-invasive brain recordings.](#) *Nature Machine Intelligence*, 5(10):1097–1107. 598 599
600 Christian Herff, Dominic Heger, Adriana De Pestors, Dominic Telaar, Peter Brunner, Gerwin Schalk, and
601 Tanja Schultz. 2015. Brain-to-text: decoding spoken phrases from phone representations in the brain.
602 *Frontiers in neuroscience*, 9:217. 603 604
605 Sepp Hochreiter and Jürgen Schmidhuber. 1997. [Long short-term memory.](#) *Neural Comput.*, 9(8):1735–
606 1780. 607
608 Nora Hollenstein, Jonathan Rotsztein, Marius Troendle, Andreas Pedroni, Ce Zhang, and Nicolas Langer.
609 2018. Zuco, a simultaneous eeg and eye-tracking resource for natural sentence reading. *Scientific data*,
610 5(1):1–13. 611 612
613 Mike Lewis, Yinhan Liu, Naman Goyal, Marjan Ghazvininejad, Abdelrahman Mohamed, Omer Levy,
614 Veselin Stoyanov, and Luke Zettlemoyer. 2020. [BART: denoising sequence-to-sequence pre-training for natural language generation, translation, and comprehension.](#) In *Proceedings of the 58th Annual Meeting of the Association for Computational Linguistics*, pages 7871–7880. 615 616 617 618 619 620
621 Chin-Yew Lin. 2004. Rouge: A package for automatic evaluation of summaries. In *Text summarization branches out*, pages 74–81. 622 623
624 Yulong Liu, Yongqiang Ma, Guibo Zhu, Haodong Jing, and Nanning Zheng. 2024. See through their minds: Learning transferable neural representation from cross-subject fmri. *arXiv preprint arXiv:2403.06361*. 625 626 627
628 Joseph G Makin, David A Moses, and Edward F Chang. 2020. Machine translation of cortical activity to text with an encoder–decoder framework. *Nature neuroscience*, 23(4):575–582. 629 630 631
632 David A Moses, Sean L Metzger, Jessie R Liu, Gopala K Anumanchipalli, Joseph G Makin, Pengfei F Sun, Josh Chartier, Maximilian E Dougherty, Patricia M Liu, Gary M Abrams, et al. 2021. Neuroprosthesis for decoding speech in a paralyzed person with anarthria. *New England Journal of Medicine*, 385(3):217–227. 633 634 635 636 637 638
639 Samuel A Nastase, Yun-Fei Liu, Hanna Hillman, Asieh Zadbood, Liat Hasenfratz, Neggin Keshavarzian, Janice Chen, Christopher J Honey, Yaara Yeshurun, Mor Regev, et al. 2021. The “narratives” fmri dataset for evaluating models of naturalistic language comprehension. *Scientific data*, 8(1):250. 640 641 642 643 644
645 Uta Noppeney and Cathy J Price. 2004. An fmri study of syntactic adaptation. *Journal of Cognitive Neuroscience*, 16(4):702–713. 646 647
648 Jerrin Thomas Panachakel and Angarai Ganesan Ramakrishnan. 2021. Decoding covert speech from eeg—a comprehensive review. *Frontiers in Neuroscience*, 15:392. 649 650 651

652 Kishore Papineni, Salim Roukos, Todd Ward, and Wei-
653 Jing Zhu. 2002. [Bleu: a method for automatic evaluation of machine translation](#). In *Proceedings of the 40th Annual Meeting of the Association for Computational Linguistics*, pages 311–318. ACL.

657 Jingyuan Sun, Shaonan Wang, Jiajun Zhang, and
658 Chengqing Zong. 2019. [Towards sentence-level brain decoding with distributed representations](#). In *The Thirty-Third AAAI Conference on Artificial Intelligence*, pages 7047–7054. AAAI Press.

662 Jerry Tang, Amanda LeBel, Shailee Jain, and Alexander G Huth. 2023. Semantic reconstruction of continuous language from non-invasive brain recordings. *Nature Neuroscience*, pages 1–9.

666 Athena Vouloumanos, Kent A Kiehl, Janet F Werker, and Peter F Liddle. 2001. Detection of sounds in the auditory stream: event-related fmri evidence for differential activation to speech and nonspeech. *Journal of Cognitive Neuroscience*, 13(7):994–1005.

671 Shizun Wang, Songhua Liu, Zhenxiong Tan, and Xinchao Wang. 2024. Mindbridge: A cross-subject brain decoding framework. *arXiv preprint arXiv:2404.07850*.

675 Zhenhailong Wang and Heng Ji. 2022. [Open vocabulary electroencephalography-to-text decoding and zero-shot sentiment classification](#). In *Thirty-Sixth AAAI Conference on Artificial Intelligence*, pages 5350–5358. AAAI Press.

680 Nuwa Xi, Sendong Zhao, Haochun Wang, Chi Liu, Bing Qin, and Ting Liu. 2023. [Unicorn: Unified cognitive signal reconstruction bridging cognitive signals and human language](#). In *Proceedings of the 61st Annual Meeting of the Association for Computational Linguistics (Volume 1: Long Papers), ACL 2023, Toronto, Canada, July 9-14, 2023*, pages 13277–13291. Association for Computational Linguistics.

688 Ziyi Ye, Qingyao Ai, Yiqun Liu, Min Zhang, Christina Lioma, and Tuukka Ruotsalo. 2023. Language generation from human brain activities. *arXiv preprint arXiv:2311.09889*.

692 Shuxian Zou, Shaonan Wang, Jiajun Zhang, and Chengqing Zong. 2021. Towards brain-to-text generation: Neural decoding with pre-trained encoder-decoder models. In *NeurIPS 2021 AI for Science Workshop*.

697 A Implementation Details

698 We apply the “Narratives” (Nastase et al., 2021)
699 dataset for fMRI-to-text decoding and the ZuCo
700 (Hollenstein et al., 2018) dataset for EEG-to-text
701 decoding in experiments. The “Narratives” dataset
702 contains fMRI data from 345 subjects listening to
703 27 diverse stories. Since the data collection process
704 involves different machines, we only consider
705 fMRI data with $64 \times 64 \times 27$ voxels. The ZuCo

706 dataset includes 12 healthy adult native English
707 speakers reading English text for 4 to 6 hours. It
708 contains simultaneous EEG and Eye-tracking data.
709 The reading tasks include Normal Reading (NR)
710 and Task-specific Reading (TSR) extracted from
711 movie views and Wikipedia. Both datasets are split
712 into training, validation, and test set with a ratio of
713 80%, 10%, 10% in all experiments.

714 More details in experiments are supplemented in
715 this section. We perform the same filtering steps to
716 “Narratives” dataset as UniCoRN paper (Xi et al.,
717 2023) and the same filtering steps to ZuCo1.0 as
718 EEG2Text paper (Wang and Ji, 2022). In BSLR
719 and TSLR calculation, the number of four different
720 seeds are set as 1, 2, 3, 4 respectively. In signal
721 reconstruction task for encoder of UniCoRN, the
722 batch size of EEG and fMRI data is 512 and 320
723 respectively. The learning rate is set as $1e-4$ and
724 $1e-3$ separately as the author claimed in the original
725 paper. In the fair benchmark, for fMRI data, en-
726 coder of UniCoRN is trained through $1e-4$ learning
727 rate and decaying to $1e-6$ finally for 30 training
728 epochs. Decoder is trained through $1e-4$ learning
729 rate and decaying to $1e-6$ finally for 10 training
730 epochs with 90 batch size. Sample length L is set
731 as 10 for all experiments related to fMRI. For EEG
732 data, EEG2Text model is trained with $1e-6$ learning
733 rate for 80 epochs. UniCoRN model is trained with
734 the same settings as fMRI data.

735 B Details of Cross-Subject Splitting

736 For fMRI dataset, we consider a bipartite graph
737 $\mathcal{G}_1 = (\mathcal{U}, \mathcal{V}, \mathcal{E})$ where $\mathcal{U} = \{S_i\}_{i=1}^N$, $\mathcal{V} =$
738 $\{M_k\}_{k=1}^M$. \mathcal{E} is the edge between node in \mathcal{U}
739 and node in \mathcal{V} , indicating $\langle S_i, M_k \rangle$ pair in the dataset.
740 N is the total number of subjects and M is the
741 total number of tasks. We assert $M < N$, so
742 $e = (u, v) \in \mathcal{E}$ exists for every $v \in \mathcal{V}$, as each
743 text stimuli is listened or read by at least one sub-
744 ject. As shown in step 2 of Figure 3, first we pick
745 one edge for each node $v \in \mathcal{V}$ and build a new
746 bipartite graph $\mathcal{G}_2 = (\mathcal{U}, \mathcal{V}, \mathcal{E}')$. Then following
747 step 3, we split graph \mathcal{G}_2 by subject \mathcal{U} with the
748 given splitting ratio and form three disjoint graphs
749 $\mathcal{G}_{train}, \mathcal{G}_{val}, \mathcal{G}_{test}$. In step 4, some edges satisfy-
750 ing zero data leakage condition are not included
751 in the graph. We add these edges to correspond-
752 ing graphs, extending each graph $\mathcal{G}_{train}, \mathcal{G}_{val}, \mathcal{G}_{test}$
753 to its maximally scalable state and finishing the
754 dataset splitting process.

755 We also release the pseudo-code of two dataset

756 splitting methods for EEG and fMRI signal. As
757 shown in Figure 3, our proposed dataset splitting
758 method consists of four steps. The blue lines stand
759 for the situation of original dataset. The main dif-
760 ference between two methods lies in the how \mathcal{G}_2 is
761 generated. We always choose the side with fewer
762 nodes in bipartite graph \mathcal{G}_1 to perform \mathcal{G}_2 genera-
763 tion. For example, in Algorithm 1 where we assert
764 $|\mathcal{U}| < |\mathcal{V}|$, the adjacency matrix is initialized as
765 $M \times N$. In Algorithm 2 where $|\mathcal{V}| < |\mathcal{U}|$, the adja-
766 cency matrix is initialized as $N \times K$. All assertions
767 are based on analysis of cognitive datasets.

768 One more thing to notice is that in Line 14 of
769 both pseudo-code, the loop indicates extending
770 training set, validation set, and test set respectively.
771 So the names of variable should be alternated in the
772 repeat loop and the displayed part in pseudo-cod is
773 a case example of extending training set. We write
774 it in this way for simplicity of expression.

Algorithm 1: Dataset splitting method for EEG signal

```
1 Initialize: Bipartite graph  $\mathcal{G}_1 = (\mathcal{U}, \mathcal{V}, \mathcal{E})$ ,  $\mathcal{G}_2 = (\mathcal{U}, \mathcal{V}, \mathcal{E}')$  where  $\mathcal{U} = \{S_i\}_{i=1}^N$  and  $\mathcal{V} = \{T_j\}_{j=1}^M$ ,  
Adjacency matrix  $A_1$  of  $\mathcal{G}_1$  where  $A_1[i][j] = 1$  if node  $i$  and node  $j$  is connected else  $A_1[i][j] = 0$ ,  
Adjacency matrix  $A_2$  of  $\mathcal{G}_2$  where  $A_2[i][j] = 0$ , Array  $C$  where  $len(C) = len(\mathcal{U})$  and  $C[i] = 0$ ;  
2 for  $u \leftarrow U_1$  to  $U_N$  do  
3    $C_{copy} \leftarrow C$ ;  
4   for  $v \leftarrow A_1[u][0]$  to  $A_1[u][M]$  do  
5     if  $v = 0$  then  
6        $C_{copy}[v.index] \leftarrow \infty$ ;  
7      $Minimum = \min(C_{copy})$ ;  
8      $A_2[u][Minimum.index] \leftarrow 1$ ;  
9      $C[Minimum.index] \leftarrow C[Minimum.index] + 1$ ;    // Make degree of nodes balanced  
10 Split by subjects  $\mathcal{U}$  according to default ratio;  
11  $\mathcal{G}_2 = \mathcal{G}_{train} \cup \mathcal{G}_{val} \cup \mathcal{G}_{test}$ ,  $\mathcal{U}_{train} \cap \mathcal{U}_{val} \cap \mathcal{U}_{test} = \emptyset$ ,  $\mathcal{V}_{train} \cap \mathcal{V}_{val} \cap \mathcal{V}_{test} = \emptyset$ ;  
12 repeat    // To three sets respectively, below is for training set  
13   for  $u$  in  $\mathcal{U}$  do  
14     for  $v$  in  $\mathcal{V}$  do  
15       if  $e = (u, v) \in \mathcal{E}$  and  $e = (u, v) \notin \mathcal{E}'_{train}$  and  $u \notin \mathcal{U}_{val} \cup \mathcal{U}_{test}$  then  
16          $\mathcal{E}'_{train} \leftarrow \mathcal{E}'_{train} \cup \{e\}$ ;  
17 until  $\mathcal{G}_{train}, \mathcal{G}_{val}, \mathcal{G}_{test}$  are all extended;  
18 return  $\mathcal{G}_{train}, \mathcal{G}_{val}, \mathcal{G}_{test}$ ;
```

Algorithm 2: Dataset splitting method for fMRI signal

```
19 Initialize: Bipartite graph  $\mathcal{G}_1 = (\mathcal{U}, \mathcal{V}, \mathcal{E})$ ,  $\mathcal{G}_2 = (\mathcal{U}, \mathcal{V}, \mathcal{E}')$  where  $\mathcal{U} = \{S_i\}_{i=1}^N$ ,  $\mathcal{V} = \{M_k\}_{k=1}^K$ ,  
Adjacency matrix  $A_1$  of  $\mathcal{G}_1$  where  $A_1[i][j] = 1$  if node  $i$  and node  $j$  is connected else  $A_1[i][j] = 0$ ,  
Adjacency matrix  $A_2$  of  $\mathcal{G}_2$  where  $A_2[i][j] = 0$ , Array  $C$  where  $len(C) = len(\mathcal{V})$  and  $C[i] = 0$ ;  
20 for  $v \leftarrow V_1$  to  $V_K$  do  
21    $C_{copy} \leftarrow C$ ;  
22   for  $u \leftarrow A_1[v][0]$  to  $A_1[v][K]$  do  
23     if  $u = 0$  then  
24        $C_{copy}[u.index] \leftarrow \infty$ ;  
25      $Minimum = \min(C_{copy})$ ;  
26      $A_2[v][Minimum.index] \leftarrow 1$ ;  
27      $C[Minimum.index] \leftarrow C[Minimum.index] + 1$ ;    // Make degree of nodes balanced  
28 Split by tasks  $\mathcal{V}$  according to default ratio;  
29  $\mathcal{G}_2 = \mathcal{G}_{train} \cup \mathcal{G}_{val} \cup \mathcal{G}_{test}$ ,  $\mathcal{U}_{train} \cap \mathcal{U}_{val} \cap \mathcal{U}_{test} = \emptyset$ ,  $\mathcal{V}_{train} \cap \mathcal{V}_{val} \cap \mathcal{V}_{test} = \emptyset$ ;  
30 repeat    // To three sets respectively, below is for training set  
31   for  $v$  in  $\mathcal{V}$  do  
32     for  $u$  in  $\mathcal{U}$  do  
33       if  $e = (u, v) \in \mathcal{E}$  and  $e = (u, v) \notin \mathcal{E}'_{train}$  and  $v \notin \mathcal{V}_{val} \cup \mathcal{V}_{test}$  then  
34          $\mathcal{E}'_{train} \leftarrow \mathcal{E}'_{train} \cup \{e\}$ ;  
35 until  $\mathcal{G}_{train}, \mathcal{G}_{val}, \mathcal{G}_{test}$  are all extended;  
36 return  $\mathcal{G}_{train}, \mathcal{G}_{val}, \mathcal{G}_{test}$ ;
```
